

..... PURPOSE OF THE CENTER  
Information Center is to provide  
broadest dissemination possi-  
of information contained in  
E's Research and Development  
ports to business, industry, the  
ademic community, and federal,  
te and local governments.

Although a small portion of this  
ort is not reproducible, it is  
ng made available to expedite  
availability of information on the  
earch discussed herein.

LA-UR-84-870  
CONF - 840255 --19

PORTIONS OF THIS REPORT ARE ILLEGIBLE. It  
has been reproduced from the best available  
copy to permit the broadest possible avail-  
ability.

Los Alamos National Laboratory is operated by the University of California for the United States Department of Energy under contract W-7405-ENG-36.

LA-UR--84-870

DE84 010054

**TITLE: INTERNAL MAGNETIC FIELD MEASUREMENTS IN A TRANSLATING  
FIELD-REVERSED CONFIGURATION**

**AUTHOR(S): W. T. Armstrong, R. E. Chrien, K. F. McKenna, D. J. Rej  
E. G. Sherwood, R. E. Siemon, M. Tuszewski**

**SUBMITTED TO: 6th U. S. SYMPOSIUM ON COMPACT TOROID RESEARCH  
February 20-23, 1984 - Princeton, NJ**

**MASTER**

**DISCLAIMER**

This report was prepared as an account of work sponsored by an agency of the United States Government. Neither the United States Government nor any agency thereof, nor any of their employees, makes any warranty, express or implied, or assumes any legal liability or responsibility for the accuracy, completeness, or usefulness of any information, apparatus, product, or process disclosed, or represents that its use would not infringe privately owned rights. Reference herein to any specific commercial product, process, or service by trade name, trademark, manufacturer, or otherwise does not necessarily constitute or imply its endorsement, recommendation, or favoring by the United States Government or any agency thereof. The views and opinions of authors expressed herein do not necessarily state or reflect those of the United States Government or any agency thereof.

By acceptance of this article, the publisher recognizes that the U.S. Government retains a nonexclusive, royalty-free license to publish or reproduce the published form of this contribution, or to allow others to do so, for U.S. Government purposes.

The Los Alamos National Laboratory requests that the publisher identify this article as work performed under the auspices of the U.S. Department of Energy.

**Los Alamos** Los Alamos National Laboratory  
Los Alamos, New Mexico 87545

## INTERNAL MAGNETIC FIELD MEASUREMENTS IN A TRANSLATING FIELD-REVERSED CONFIGURATION\*

W. T. Armstrong, R. E. Chrien, K. P. McKenna, D. J. Rej,  
E. G. Sherwood, R. E. Siemon and M. Tuszewski

- Los Alamos National Laboratory, Univ. of California, Los Alamos, NM 87545

-I. INTRODUCTION: Magnetic field probes have been employed to study the internal field structure of Field-Reversed Configurations (FRCs) translating past the probes in the FRX-C/T device.<sup>1</sup> Internal closed flux surfaces can be studied in this manner with minimal perturbation because of the rapid transit of the plasma (translational velocity  $v_z \sim 10 \text{ cm}/\mu\text{s}$ ). Data have been taken using a low-field (5 kG), 5-mtorr-D<sub>2</sub> gas-puff mode of operation in the FRC source coil which yields an initial plasma density of  $\sim 1 \times 10^{15} \text{ cm}^{-3}$  and  $x_s \sim 0.40$ . FRCs translate from the  $\sim 25 \text{ cm}$  radius source coil into a  $20 \text{ cm}$  radius metal translation vessel. Two translation conditions are studied: 1) translation into a 4 kG guide field ("matched guide-field" case), resulting in similar plasma parameters but with  $x_s \sim 0.45$ , and 2) translation into a 1 kG guide field ("reduced guide-field" case), resulting in expansion of the FRC to conditions of density  $\sim 3 \times 10^{14}$ , external field  $B_0 \sim 2 \text{ kG}$  and  $x_s \sim 0.7$ . The expected reversed  $B_z$  structure is observed in both cases. However, the field measurements indicate a possible sideways offset of the FRC from the machine axis in the matched case. There is also evidence of island structure in the reduced guide-field case. Fluctuating levels of  $B_\theta$  are observed with amplitudes  $< B_0/3$  in both cases. Field measurements on the FRC symmetry axis in the reduced guide-field case indicate  $\beta$  on the separatrix of  $B_s \sim 0.3$  (indexed to the external field) has been achieved. This decrease of  $B_s$  with increased  $x_s$  is expected, and desirable for improved plasma confinement.

II. EXPERIMENTAL ARRANGEMENT: The probes consist of two separate sets of multi-turn wire loops housed within 5/16" O.D., s.s. jackets which result in 300 ns response times. One three-axis probe is positioned on the symmetry axis of the device for reference while the other three-axis probe is scanned radially on a shot-to-shot basis. The probes are located  $\sim 1.9 \text{ m}$  beyond the end of the 2 m long FRC formation coil, in a uniform dc field region, and  $\sim 1.5 \text{ m}$  before a magnetic mirror region ( $z_{\text{probe}} = 293 \text{ cm}$  in Fig. 1 of ref. 1). Fixed  $B_z$  probes external to the FRC and interferometry measurements at approximately the same axial location as the internal probes, are used to aid in the analysis of the internal field measurements.

The probe jackets have an "L" shape: entering the vacuum vessel radially, turning at the probing radius  $90^\circ$  towards the  $-z$  direction (direction of oncoming FRC) and terminating at the probe location  $\sim 8 \text{ cm}$  from the  $90^\circ$  bend. This jacket shape allows for minimal perturbation of the plasma's azimuthal diamagnetic current at the axial location of the probe. Other perturbations, plasma cooling and increased electron density from impurities, are anticipated to be minimal due to the small surface area of the probe jacket, but none-the-less increasing as the FRC traverses the probe. A global check of field similarity with and without probing is made by comparing radius histories of the translating FRC at two axial locations prior to the probing location with the radius history at the probe location. This comparison shows that only the trailing portion of the FRC at the probing location departs from the earlier histories. This variation may result from increasing perturbation of the FRC by the probes as mentioned above, or from the FRC slowing due to its encountering of the magnetic mirror downstream. These dissimilar data are not analyzed.

A summary of plasma parameters for the source and the two translation cases is given in Table I (source parameters differ slightly from those of Ref. 1 for this particular data run, resulting in higher translation velocities). The inferred parameters are: the "volume" averaged density  $\bar{n} = \int n dl / r_s$ , the total temperature  $T = \bar{B} B_0^2 / 8\pi\bar{n}$ , the separatrix radius  $r_s$  = excluded flux radius, the internal flux  $\Phi_i = B_0 r_w x_s^{3.25}$ , and the volume averaged beta  $\bar{\beta} = 1 - x_s^2/2$ . Since  $\bar{n}$  is not a true volume averaged quantity,  $\bar{n}$  and  $T$  are estimates to approximately 10% accuracy. The source FRC's magnetic field and radius are measured 15 cm from the source-coil midplane in the direction of translation. Note in the Table that due to acceleration in the conical source coil, and due to the high translation velocity in the reduced guide-field case, the FRC may not have full equilibrium conditions. Departure from full equilibrium may introduce additional error in some inferred parameters. Finally, the stable period before the rotational instability occurs in both translation cases, is  $> 40 \mu s$  so that the  $n = 2$  elliptical deformation is not expected to affect interpretation of the data.

**III. MATCHED GUIDE-FIELD TRANSLATION:** Axial profiles of B-fields, density and radius for three similar shots are displayed in Fig. 1. Translation velocities for each shot have been used to convert time histories to axial profiles. Figure 1a displays the excluded flux radius and line-integrated density (double pass) overlaid for the three shots. Figure 1b shows the reference external field and  $B_z$  field measured on the machine axis for the three shots.  $B_z$  fields at three intermediate radii (each radii is from a different shot) are also shown in Fig. 1b. The expected reversal of  $B_z$  with radius is evident in the figure. Figure 1c displays the  $B_r$  and  $B_\theta$  field components (with respect to the machine axis) for the three radial positions scanned in the three shots. The  $B_\theta$  amplitude ( $< B_0/3$ ) results in  $< 11\%$  contribution to pressure balance. Furthermore, the small  $B_\theta$  amplitude together with its fluctuating structure is distinctly different from that of a Spheromak. A possible explanation for the existence of  $B_\theta$  is the presence of "torsional-Alfven" waves generated by the axial acceleration of the FRC out of the shallow conical theta-pinch source region.<sup>2</sup> Also, tilting and sideways offset of the FRC may contribute to pickup of  $B_r$  and  $B_z$  on the  $B_\theta$  probe.

A radial scan of  $B_z$  is presented in Fig. 2 in which data were averaged over three shots and over 40 cm axial extent centered at the FRC midplane. The data is consistent with a sideways offset of the FRC of  $\Delta x \sim 1.5$  cm along the probing diameter. Furthermore, comparison with theoretically predicted  $B_z(r)$  profiles<sup>3</sup> assuming  $x_s = 0.45$  and  $\beta_s = 0.7$  (based on long-thin equilibrium constraints) indicates the measured  $B_z$  radial profile is narrower than predicted. This difference may be explained by a further sideways offset of the FRC  $\Delta y \sim 4$  cm perpendicular to the probing diameter (inferred offset is not sensitive to choice of  $\beta$ ). With these offsets, the probing radii indexed to the coil center of -4.3, 0.0, +4.0 and +8.0 cm become probing radii along a chord indexed to the FRC center of -4.9, 4.3, 6.8 and 10.3 cm, respectively. This adjusted scale is indicated at the top of Fig. 2.

**IV. REDUCED GUIDE-FIELD TRANSLATION:** Axial profiles of plasma parameters are presented in Fig. 3, again for three shots, in which the plasma expanded into an initial guide field of  $\sim 1$  kG. As in Fig. 1, the field measurements at three intermediate radii represent a different probe placement on each shot. Field reversal similar to the previous case is observed. However, the radial extent of the reversal region is considerably broader as indicated by similar  $B_z$  values from 0 to 8 cm radius. Evidence of island formation is seen in the oscillation

$r_{\Delta\phi}(z)$  profiles. From full, FRC  $r_{\Delta\phi}(z)$  profile histories, the presence of partially merged FRCs can be seen starting in the source coil. Multiple FRC island structure in  $r_{\Delta\phi}(z)$  profiles has also been observed in 2-D simulations.<sup>4</sup> A possible cause of the multiple island structure in the present translation experiments may be the strong accelerating field gradient at the edge of the source coil which is present with a reduced guide field. As the plasma passes through this step in  $B_z$ , the leading plasma will be accelerated away from the trailing plasma, enhancing any initial island structure that may be present after FRC formation.

A radial profile of  $B_z$  is shown in Fig. 4, in which the averaging method of Fig. 2 is used. Also shown in the figure is a profile theoretically predicted from equilibrium constraints,<sup>3</sup> for  $x_s = 0.7$  and  $\beta_s = 0.3$ . Good agreement is found between the two profiles, with the experimental data indicating a slightly wider reversed field region (corresponding to a more peaked pressure profile at the field null). The expected low  $\beta_s$  for large  $x_s$  is observed in the data. Low  $\beta_s$  is important for obtaining improved plasma confinement in FRCs. No sideways offset of the FRC is indicated by the data. In Table I the internal reversed flux  $\Phi_i$ , inferred from equilibrium constraints, is larger in the expanded translated FRC compared to the source or matched translation FRC. The source  $\Phi_i$  may be underestimated due to the lack of full equilibrium conditions. However, the  $\Phi_i$  downstream is measured independently by the internal probe measurements to be in the range of 275-350 kG cm<sup>2</sup>, in support of the large, global  $\Phi_i$  estimate in the table.

---

\*Work supported by the U.S. Department of Energy

References:

1. D. J. Rej, et al., these proceedings.
2. D. W. Hewett, accepted to Nuclear Fusion.
3. D. W. Hewett and R. L. Spencer, Phys. Fl. 26, 1299 (1983).
4. W. T. Armstrong and R. D. Milroy, Proc. of the Fifth Symp. on the Phys. and Tech. of Compact Toroids, (Bellevue, 1983) ,1; and R. D. Milroy, private communication.

TABLE I  
Plasma Parameters

Source ( $t=10\mu s$ )	Matched guide-field translation ( $t=40\mu s$ )	Reduced guide-field translation ( $t=30\mu s$ )
$B_0$ (kG) $\bar{n}$ ( $10^{15} \text{cm}^{-3}$ )	5.5 1.1	4.8 .9
T (eV)	630	540
$\Phi_i$ (kG cm <sup>2</sup> )	175	140
$r_s$ (cm)	10	9.2
$l_s$ (cm)	150	180
$x_s$	.4	.45
$\beta$	.92	.90
$v_z$ (cm/ $\mu s$ )	--	12
$v_A$ (cm/ $\mu s$ )	25	23
$N$ ( $10^{19}$ )	6.1	4.5
$(3/2)NT$ (kJ)	8.0	5.5
$Mv_z^2/2$ (kJ)	--	1.1
$E_{\text{kin}}$ (kJ)	8.0	7.0

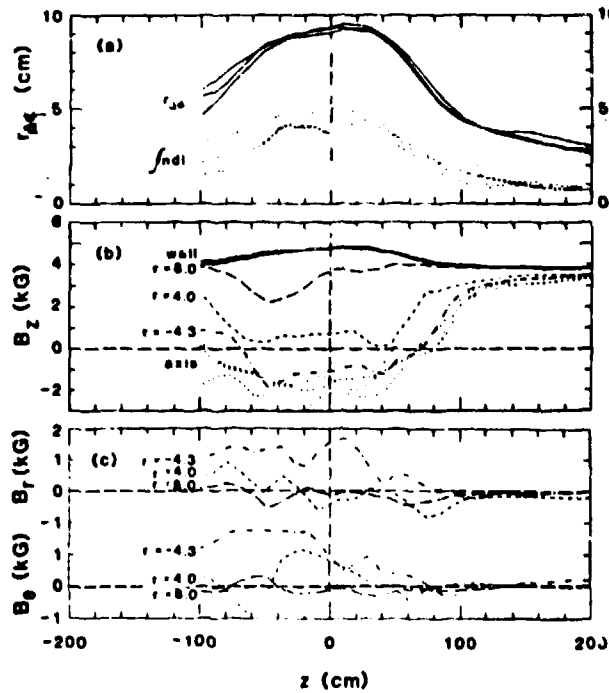


Figure 1. Matched guide field data:  
a)  $r_{\Delta\phi}$  and  $f_{ndl}$  (double pass)  
b)  $B_z$  at different coil radii; coil  
axis (dotted),  $r = -4.3$  cm (dot-dash),  
 $r = 4.0$  cm (short dash),  $r = 8.0$  cm  
(long dash), wall (solid), c)  $B_r$   
and  $B_\theta$  at same positions as in b).

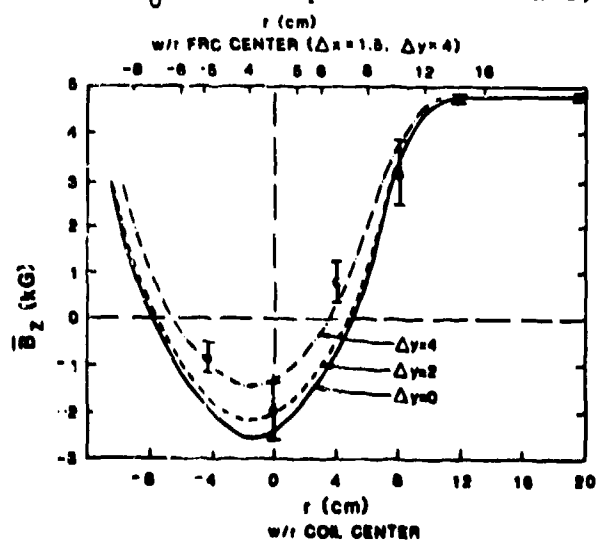


Figure 2. Average  $B_z$  vs  $r$  for matched  
guide-field case. Error bars are rms  
deviations. Theoretical profiles are  
shown for FRC offsets from the probing  
diameter of 0, 2 and 4 cm. Inferred  
probing radii w/r to FRC major axis  
are shown at top.

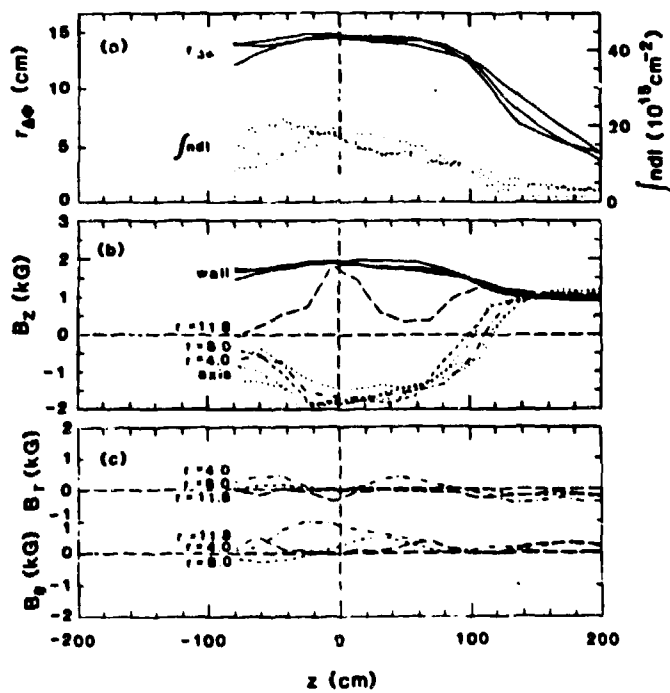


Figure 3. Reduced guide-field data:  
a)  $r_{\Delta\phi}$  and  $f_{ndl}$  (double pass)  
b)  $B_z$  at different coil radii; coil  
axis (dotted)  $r = 4.0$  cm (dot-dash),  
 $r = 8.0$  cm (short dash),  $r = 11.8$  cm  
(long dash), wall (solid), c)  $B_r$   
and  $B_\theta$  at same positions as in b).

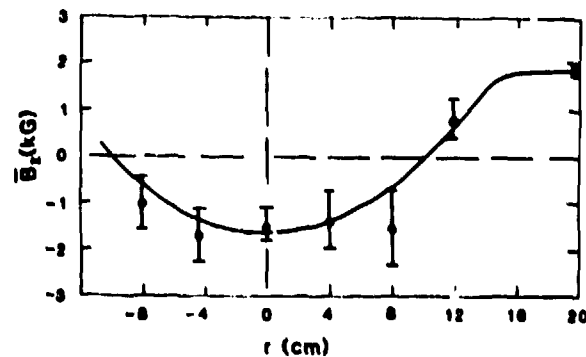


Figure 4. Average  $B_z$  vs  $r$  for  
reduced guide-field case.  
Error bars are rms deviation.  
Theoretical profile is solid curve.